A growth model for eucalypt in Galicia, Spain

Oscar García [a,1], Federico Ruiz F. [b]

[a] *University of Northern British Columbia, 3333 University Way, Prince George, B. C., Canada V2N 4Z9*

[b] *CIT – ENCE, Apartado de Correos 223, 21080 Huelva, Spain*

Abstract

A relatively simple system of differential equations was used for predicting growth of eucalypt coppice stands. Only limited, low quality data was available, from small continuous forest inventory plots not originally designed for growth modelling. Therefore, biological principles and growth patterns observed elsewhere were used to constrain model form. The differential equations used are analytically integrable, facilitating usage and estimation. Similar models and techniques may be useful in other data-poor situations.

Key words: *Eucalyptus globulus*, coppice, site index, differential equations, multivariate Richards, occupancy

1 Introduction

Introduced into Europe from Australia around the middle of the 19th century, *Eucalyptus globulus* Labill is widespread at the lower elevations along the Western and Northern coasts of the Iberian Peninsula. In Galicia, North-Western Spain, it has in recent years rivaled *Pinus pinaster* as the most important commercial tree species. The only growth projection tools for Galicia, however, were two unpublished yield tables by A. Fernández López, based on temporary sample plots (Rojo and Montero, 1994; Madrigal C. et al., 1999). We have developed a stand growth model using continuous forest inventory plot measurements from the *Empresa Nacional de Celulosas* (ENCE).

The data comes from unthinned stands, thinning of eucalypts being uncommon in Galicia. Thus, it would have been feasible to limit the study to the

[1] Corresponding author. *Email address:* garcia@unbc.ca

production of traditional "static" yield functions (Alder, 1980). It was felt, however, that a dynamic model, at least beyond the early ages, would be more useful in two respects. First, there is some interest in future diversification into the production of eucalypt sawn timber, in addition to the currently predominant use for pulp and particle-board. It would be interesting, then, to estimate the response of various spacing and thinning regimes, even if on a somewhat speculative basis at this stage. Second, using static yield functions to project the future development of existing stands, which in general have deviated from the predicted trajectories due to climatic fluctuations or other causes, requires *ad hoc* approximations or adjustments of doubtful rationality and accuracy. Dynamic models deal with these issues in a natural way.

Most of the data corresponds to coppice, including spontaneous vegetative regeneration after fire, and it was found necessary to exclude planted stands from the model. The heterogeneous nature of these forests, their fast growth rates, and the small size of the sample plots, resulted in highly variable observations. Together with the limited stand density coverage, this made the use of purely empirical relationships impractical. The structure of the model, therefore, is largely based on ecophysiological considerations and previous experience with other species.

We used a relatively simple system of differential equations, integrable analytically, thus facilitating usage and parameter estimation. We believe that the model and techniques applied here are of wider methodological interest, in particular being potentially useful in other "data-poor" situations.

The structure of the article is as follows. After a brief background on the data, the top height growth and site index sub-model is described, followed by the time-scaling approach used for incorporating differences in site quality. The mortality component comes next, before being used in the development of the basal area growth equation. Then all the growth equations are brought together, and methods for computing growth projections are discussed. This dynamic model is only appropriate for closed-canopy stands, so that young stands need to be "started" with a separate initial growth estimate. Other variables of interest, such as volume per hectare, are estimated from the current values of the projected height, number of stems, and basal area. A relationship between number of stems and basal area removed in thinning is also useful. After developing these additional elements, we end with a discussion and conclusions. A modification of the model that eliminates the need for a separate estimate of initial growth is presented in the Appendix.

2 Data

The data comes from ENCE's continuous forest inventory, and consists of permanent sample plots of 200 m^2, measured between 1988 and 1994. There were 113 plots in coppice, all of them first rotation, and 20 planted plots. Each had between 1 and 5 re-measurements, mostly at one year intervals. The range of ages and other variables can be appreciated from the figures. As discussed below, only the coppice data was used in the final model.

In the inventory all live trees are counted, and diameter at breast height (dbh) and total height are recorded for those with a dbh of at least 5 cm. Volume for these trees is estimated from dbh and height with a tree volume equation. Stand top height is taken as the average of the two largest trees in the plot. Sampling and measurement methods have been described in more detail by Pardo (1990). The data ranges and distribution can be appreciated in the figures that follow.

3 Height growth and site quality

Top heights are graphed over age in Figure 1. Ages are years since planting or, in coppice, since the previous stand harvest. The growth trends show a high degree of variability. This may be largely attributed to the small plot size, to the heterogeneity typical of eucalypt stands in Galicia, and possibly to imprecision in tree height and/or stand age measurements. Although top height was based on only two trees per plot, this does not appear to be a major factor because graphing mean heights shows a similar pattern.

Growth was modelled with Richard's differential equation, which may be conveniently linearized as

$$\frac{\mathrm{d}H^c}{\mathrm{d}t} = b(a^c - H^c) \ , \tag{1}$$

where H is top height (m), t is the age (years), and a, b and c are parameters to be estimated (García, 1983). Also known as the von Bertalanffy or Chapman-Richards model, it is more commonly written as $\mathrm{d}H/\mathrm{d}t = \kappa H - \eta H^\gamma$. One of the parameters (or a combination of them obtained through reparameterization) is assumed to be site quality-dependent, being specific to each plot ("local"), while the others are common to all plots ("global").

Integration of (1) predicts H at any age t, given the height H_0 at some other

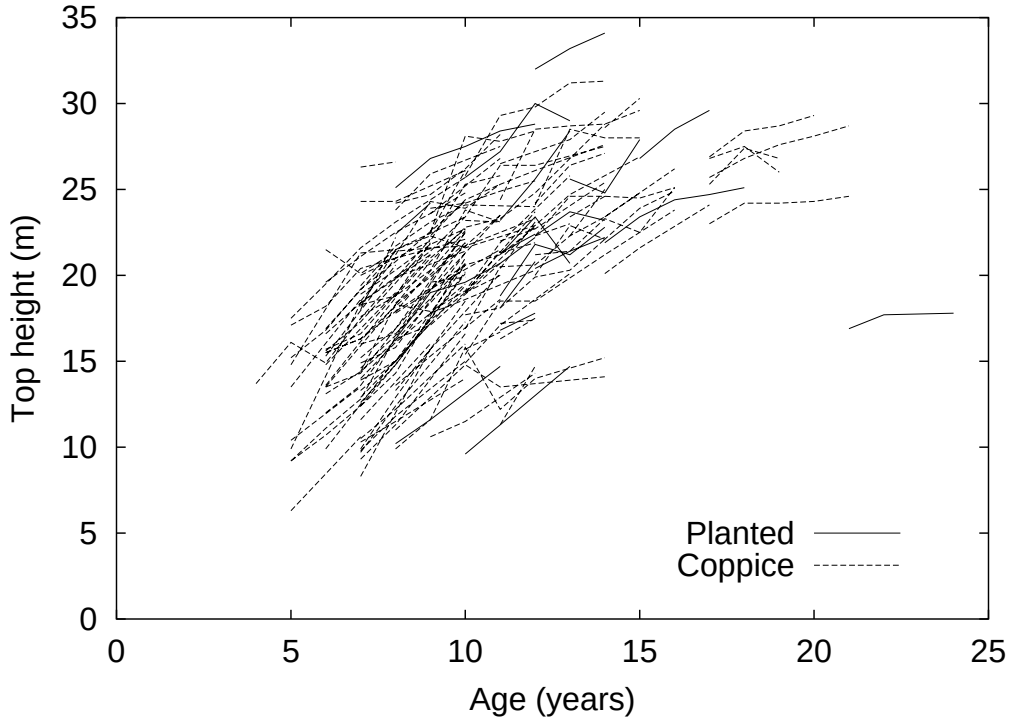

Fig. 1. Top height *vs* age. Successive measurements in the same plot are joined by lines.

age t_0:

$$H = a\{1 - [1 - (H_0/a)^c] \exp[-b(t - t_0)]\}^{1/c} . \tag{2}$$

With a fixed origin $[t_0, H_0]$, usually taken as $[0, 0]$, this expression also describes a family of *site index curves*. The family is parameterized, or indexed, by the free local parameter, that is, by the parameter chosen as varying across stands. More conventionally, a site index S can be used, defined as the top height that a "typical" stand growing in the site would reach at some base age t_c. It is related to the local site-dependent parameter through the substitution of S and t_c for H and t in (2). See García (1983) for further details and generalizations.

All the parameters, global and local, were estimated simultaneously by maximum likelihood (ML) as described in García (1983). Essentially, the method represents variability in the data by adding white noise to the right-hand side of (1), which simulates environmental fluctuations, and by including independent random measurement errors in the observed heights. The likelihood function for the resulting stochastic model is calculated, and the parameter values that maximize this function are found with a custom-built optimization algorithm. Extensive experience with the technique has proven it to be highly efficient and robust, even (or especially) in instances of scarce or poor quality data (García, 1999).

Table 1
Height growth model estimates

	Plots	Measurements	a	c	Log-likelihood
Coppice	113	388	31.60	0.6339	366.4
Planted	20	63	33.88	0.6686	78.7
Pooled	133	451	32.68	0.6808	438.6

Note that in this approach the base age is just an arbitrary reference point, a convention used for the calculation of the traditional site index. Site quality is more directly tied to the site-dependent parameter in the model, and changing the base age has no effect on the estimates or predictions. That is, the method is "base age invariant" (Bailey and Clutter, 1974). A base age $t_c = 10$ years was adopted during model development, but in the final implementation it was changed to 7 years following ENCE's preferences and practices in their other eucalypt plantations.

Two main model variants were tested, one where the site-dependent or local parameter is the height asymptote a, and another where the local parameter is the time scale factor b. The first option produces *anamorphic* curves, the effect of site being a change in the vertical H scale. The second option gives so-called *polymorphic* curves, with the horizontal time scale dependent on site. Allowing an origin different from $t = 0$ and $H = 0$ was also tried. In previous experience with the model, these have consistently been the best parameterization alternatives (García, 1999).

Bests results were obtained with b as the local parameter. Table 1 shows values of separate estimates for the coppice, the planted stands, and for the total pooled data. Here $t_0 = H_0 = 0$.

The anamorphic version gave significantly lower log-likelihoods (325.9, 71.9, and 397.8, for coppice, planted, and pooled, respectively), and fits that visually appeared clearly inferior. Including t_0 as an additional parameter in the b-local model increased the pooled log-likelihood to 438.9, not significantly different from the previous one considering the reduction in degrees of freedom. In addition, the estimated t_0 was 0.0044 years, practically zero.

The hypothesis of equality between coppice and planted can be tested by comparing the sum of the log-likelihoods to the log-likelihood for the pooled data. The difference, 6.5 units with 4 additional estimated parameters (a, c, and two variances), lies within the uncertainty margins of the various criteria available for testing the hypothesis at the 5% significance level (García, 1983, 1984). Prediction differences between the three models are relatively small, particularly within the ranges where there is sufficient data. On the other hand, the planted data is scarce and fairly variable. We cannot rule out much steeper

trends, like those observed for eucalypt plantations under similar climatic conditions in Chile where the a asymptote was estimated at 75.3 meters (García, 1995). In addition, there is evidence of eucalypts in Galicia reaching heights much larger than the asymptotes obtained here.

Given the uncertainty, and the fact that current interest focuses mainly on the growth of coppice stands, we have limited ourselves to model these. The a and c parameter estimates are therefore those in the top row of Table 1. Equation (2) reduces to

$$H = 31.60(1 - \mathrm{e}^{-\mathrm{bt}})^{1/0.6339} \; . \tag{3}$$

The site index is obtained from b by substituting the base age t_c for t. Conversely, solving for b, this value can be calculated given S:

$$b = -\ln[1 - (S/31.6)^{0.6339}]/t_c \; . \tag{4}$$

Some of the site index curves are displayed, together with the coppice data, in Figure 2.

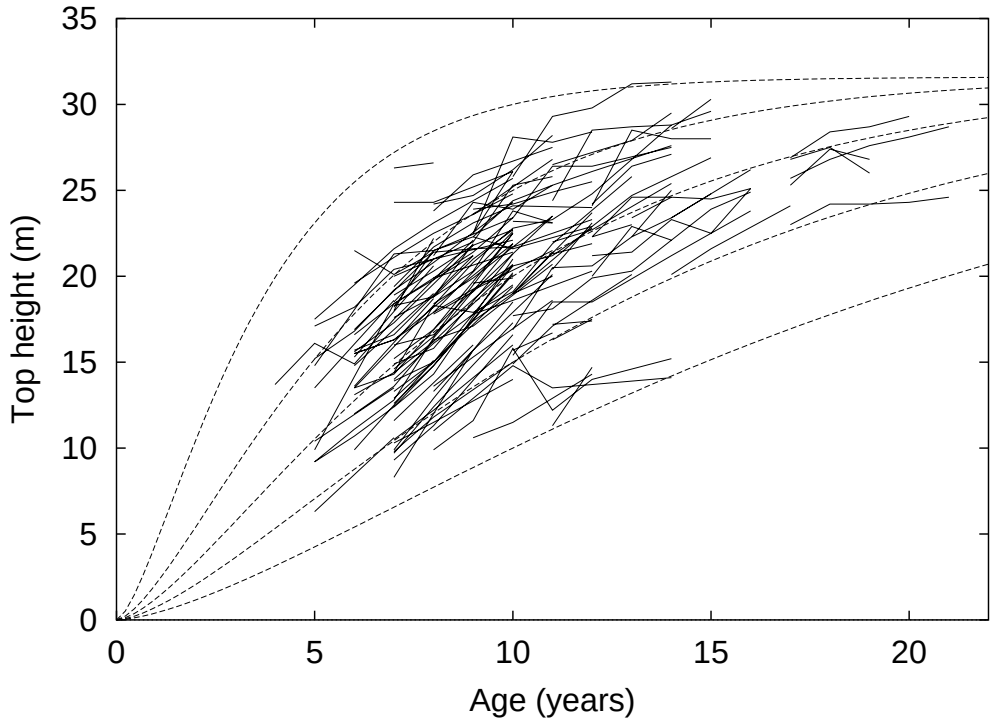

Fig. 2. Site index curves and coppice top height data

4 Site scaling

Figure 3 shows basal area over age for the available data. The large variation is in part due to differences in site quality. One simple way of accounting for site in a model is to use top height instead of age as the independent variable, assuming that relationships among stand variables other than age are not affected by site quality (e. g. Beekhuis, 1966; Mitchell, 1975; Drew and Flewelling, 1979). This slightly extends *Eichhorn's rule*, the often confirmed observation that yield tables relating stand volume to stand height tend to be the same for all sites (Eichhorn, 1904; Assmann, 1970). However, imprecision in observed stand heights can obscure trends and affect estimates.

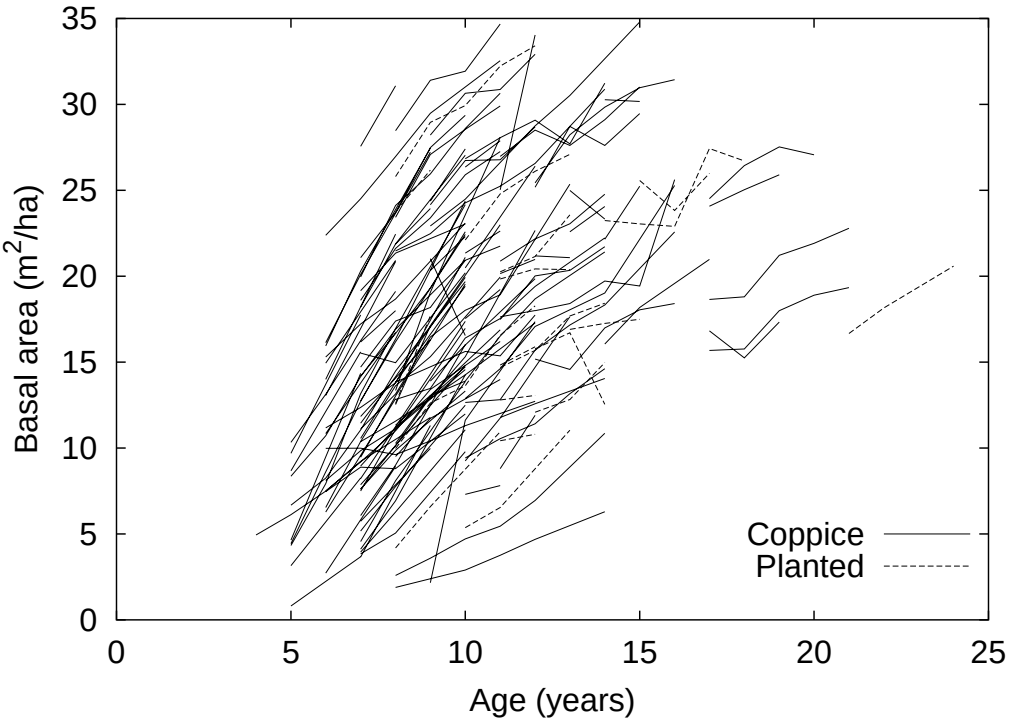

Fig. 3. Basal area over age. Same-plot measurements joined by lines.

As seen in the previous section, in this instance site quality affects top height through a change in the time scale. Therefore, a better implementation of these ideas adjusts the ages, multiplying them by some quantity proportional to the site factor b, making them "physiologically equivalent"(García, 1990). We chose to multiply all ages by $7b$, matching them to those for $b = 1/7$ or $S = 20.51$ (base age 10), a value close to the average observed site index. The ML b-estimates for each plot (local parameters) were obtained from the height model fitting procedure. In what follows, the age t refers to this adjusted or reference age. Scaling reduces data scatter substantially, although considerable variability in the increments remains (Figure 4). Color graphic plotting showed no clear residual site index effects in any of the scaled graphs.

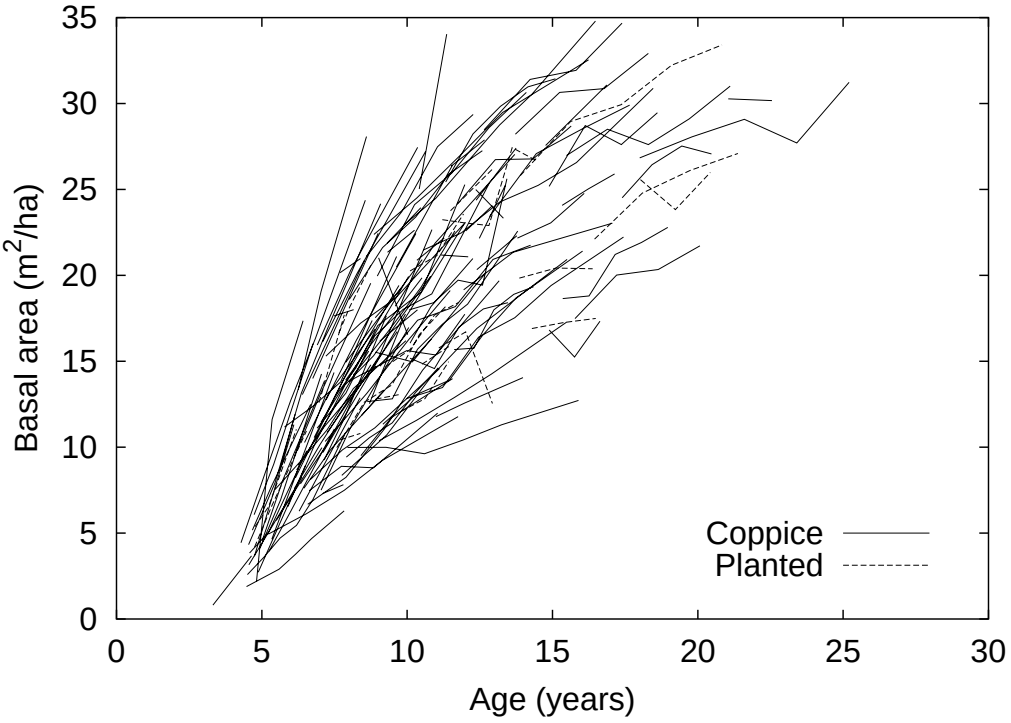

Fig. 4. Basal area over site-adjusted age.

5 Mortality

5.1 Stems per hectare

Tree mortality, even *regular mortality* which excludes severe wind damage and other catastrophic losses (Vanclay, 1994), is notoriously difficult to model, being extremely variable, greatly influenced by weather conditions, and weakly correlated with other stand characteristics (Clutter et al., 1983). The present instance is no exception (Figure 5).

As seen in figure 5, sometimes the number of stems N increases. In general, this seems to be caused by ingrowth of new sprouts or seedlings (only trees greater than 5 cm dbh were measured), which can be ignored due to their small contribution to growth and competition. Without detailed analysis of the original individual-tree raw data, it is not known if at the same time other trees died, so that the 25 intervals between successive measurements where the numbers of stems increased were eliminated. This left 250 measurement intervals available for further analysis (Figure 6).

We calculated the relative annual mortality for each interval, and looked at relating it to various stand variables. The relative mortality rate, $-(\mathrm{d}N/\mathrm{d}t)/N =$

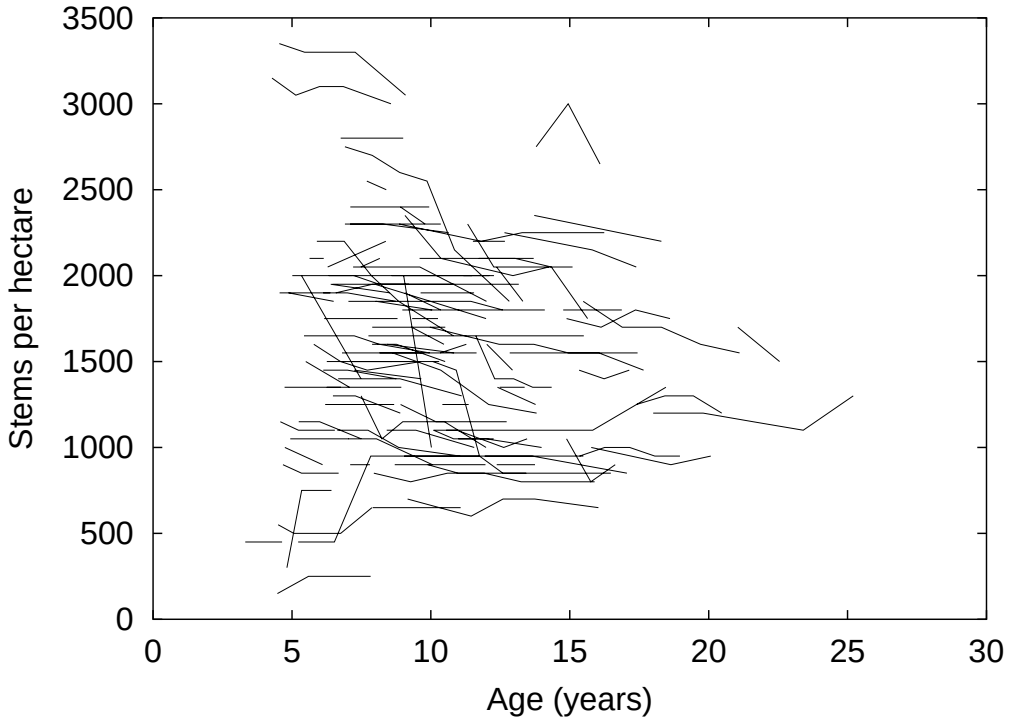

Fig. 5. Changes in the number of trees per hectare with (site adjusted) age.

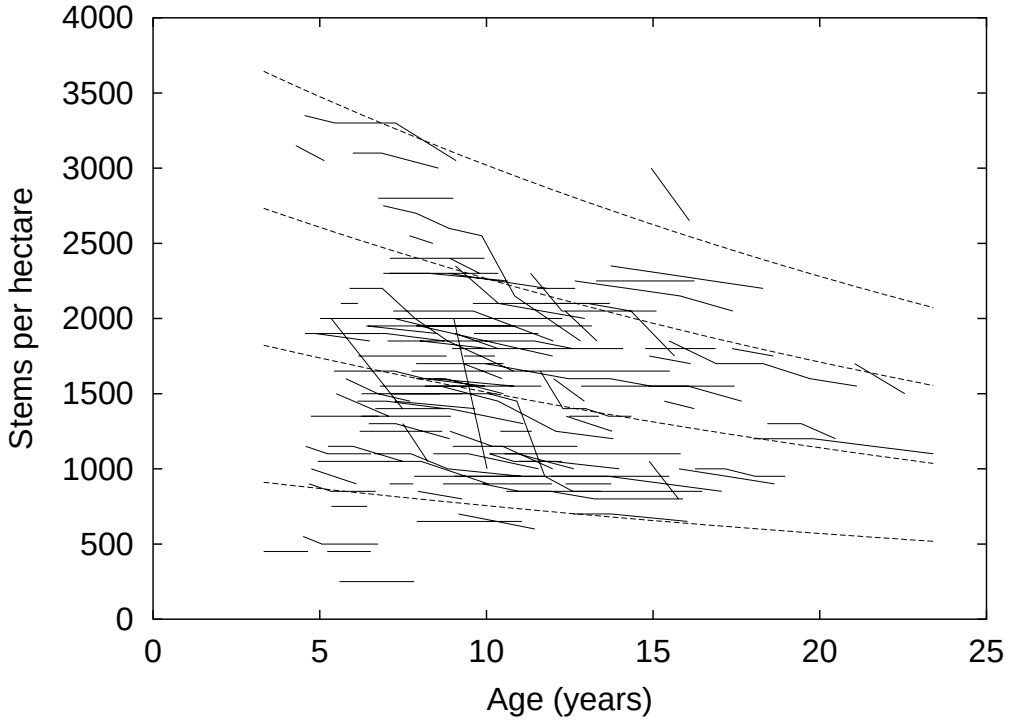

Fig. 6. Observed and predicted natural mortality. Model projections for initial stockings of 1000, 2000, 3000 and 4000 stems per hectare. Data with increasing N not included

$-\mathrm{d}\ln N/\mathrm{d}t$, was approximated by the divided differences

$$-\frac{\ln N_2 - \ln N_1}{t_2 - t_1} \ , \tag{5}$$

where N_1 and N_2 are the numbers of stems and t_1 and t_2 the site adjusted ages for two consecutive measurements. Other variables were represented by their interval averages $(x_1 + x_2)/2$.

No clear trends were apparent when plotting this relative mortality against any stand variables: t, H, N, basal area per hectare (B), mean dbh (D), volume per hectare (V). No relationships were found either with various combinations of variables, including stand density indices such as Reineke's $ND^{1.6}$ and the $V\sqrt{N}$ implicit in the *3/2 self-thinning rule* (Clutter et al., 1983; Vanclay, 1994). Therefore, we model the relative mortality rate as a constant $-\mathrm{d}\ln N/\mathrm{d}t = m$, or

$$\frac{\mathrm{d}N}{\mathrm{d}t} = -mN \ . \tag{6}$$

Integration produces estimates for the number of stems per hectare N at age t, given the number N_0 at any other age t_0:

$$N = N_0 \, \mathrm{e}^{-m(t-t_0)} \ . \tag{7}$$

Notice that in this instance (5) would equal m, in the absence of noise. A reasonable estimate for m is the mean of the observed relative mortalities, $m = 0.0281$. As a percentage of the initial number of stems, this represents an annual mortality of $100(1 - \mathrm{e}^{-0.0281}) = 2.77\%$ (for the average site). Figure 6 compares the mortality curves (7) and the data. Note, however, that mortality shortly after establishment may follow a different pattern, with different mechanisms at work; information on numbers of stems past the initial development stages should be used if possible.

5.2 Mortality in basal area and volume

In order to relate net and gross increments, we also need the mortality in terms of volume per hectare (V). It seems reasonable to approximate the mortality in V by the product of the number of dead trees and the mean tree volume, times a factor $k < 1$ to take into account the fact that dead trees tend to be smaller than average:

$$k\frac{V}{N}\frac{\mathrm{d}N}{\mathrm{d}t} \ . \tag{8}$$

Dead trees have not been measured, so there is no direct information on volume or basal area mortality. From Beekhuis (1966), however, we can derive the same relationship, and a reasonable value for k. On page 15, the periodic basal area mortality in square feet per acre for radiata pine is estimated as

$$\Delta B = 0.004158 D^2 \, \Delta N \ ,$$

where ΔN is the mortality in number of stems per acre, and D is the quadratic mean dbh in inches at the start of the measurement interval. Intervals are 2 or 3 years. Changing to metric units and substituting D in terms of B and N,

$$\Delta B = 0.7624 \frac{B}{N} \Delta N \ .$$

If V is approximately proportional to BH and, as could be expected, the top height is not affected by the dead trees, the same equation applies when substituting V for B. Except for the approximation of infinitesimal by finite intervals, this is the same as (8), with $k = 0.7624$.

It can be seen, though, that the value of k for volume should be slightly lower than that for B, because of the lower than average height of the dead trees. Beekhuis (1966, p.19) finds that in thinnings the volume-basal area ratio for the removed trees is about $2\frac{1}{2}\%$ smaller than for the initial stand, which would imply $k = 0.975 \times 0.7624 = 0.743$ for volume. It is found also that in going from finite to infinitesimal intervals k should be slightly smaller. From all this, and for lack of a better estimate, we shall use $k = 0.75$, as a reasonable figure. The exact value will not make much difference to the growth predictions.

6 Basal area and volume growth

It seems clear from Figure 4 that a purely empirical model derived exclusively from these data would not be very reliable. Variability is high, and all stands are unthinned. Many different equations could fit the observations equally well, but differ for treatments poorly represented or absent from the data base. Nevertheless, it is possible to take advantage of experiences elsewhere and of theoretical reasoning to narrow down the alternatives.

Growth in total biomass or stem volume is more easily interpreted than that in basal area or dbh, being more directly related to assimilation per unit area. We can write the net increment

$$\frac{\mathrm{d}W}{\mathrm{d}t} = \text{gross increment} - \text{mortality} \ , \tag{9}$$

where W might be biomass or volume per hectare, or a suitable proxy. Here we use the product of basal area per hectare and top height $W \equiv BH$, being more directly measurable and independent of particular tree volume tables, utilization limits, etc. W and V are strongly correlated, with $V = W/3$ being a close approximation in this instance (see below). The gross increment and mortality in (9) are in units of W per unit time.

From (8), we already have the mortality term. We need an expression for the gross increment. The gross increment is

$$\frac{\mathrm{d}W}{\mathrm{d}t} - kW\frac{\mathrm{d}\ln N}{\mathrm{d}t} \ ,$$

and we look to model it as an appropriate function of stand variables, at least for closed-canopy stands. For each pair of consecutive measurements we approximated the derivatives by the divided differences $(W_2 - W_1)/(t_2 - t_1)$ and (5). For W we used $(W_1 + W_2)/2$, and analogously for the independent variables, except for N where we preferred $\ln N \approx (\ln N_1 + \ln N_2)/2$ because of linearity (c. f. equations (6), (7)).

As a first approximation, for closed-canopy stands the gross increment could be expected to be roughly constant, assuming that assimilation efficiency, respiration or other losses do not change much with stand structure (or that they compensate for each other in terms of stem-wood increase). In fact, extensive data from radiata pine plantations subject to a wide range of treatments, and other published growth experiments, show linear trends of accumulated gross stem volume per hectare over age for closed stands, continuing up to ages far beyond normal rotations (García, 1990). The slopes appear slightly less steep on the lower lines (lower density stands). The best predictor for the gross increment in García (1990) was the number of stems per hectare, with a regression linearly decreasing with the mean spacing $1/\sqrt{N}$, and no other significant additional variables. Our graph of W *vs* t (Figure 7) is not inconsistent with this hypothesis, taking into account that there is mortality for the higher values of W, and less than full closure for low W. Using V instead of W gives very similar results.

The calculated gross increments are plotted over N in Figure 8. Only measurements with $W \geq 150$ m^3/ha (approx. $V \geq 50$ m^3/ha) were used, thus excluding slower-growing open stands (see Figure 7). Five outliers were omitted: three with high relative mortalities (0.69, 0.50, and 0.31), and two with excessively high increments. The remaining growth intervals include 93 with mortality, and 98 which did not contain any dead trees. These last ones should be somewhat more reliable, not depending on assumptions about W-mortality [2].

[2] They are still subject to considerable measurement and sampling errors, especially for top height, which in particular explains the presence of negative increments

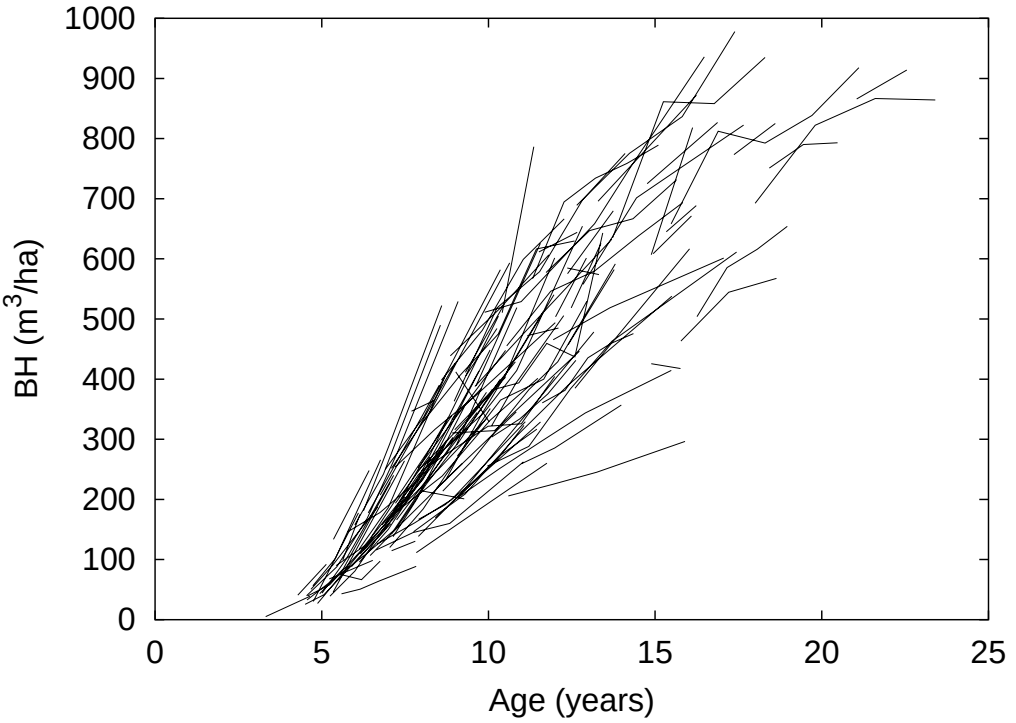

Fig. 7. W *vs* site-adjusted age. $W \equiv BH$ is approximately 3 times the volume per hectare.

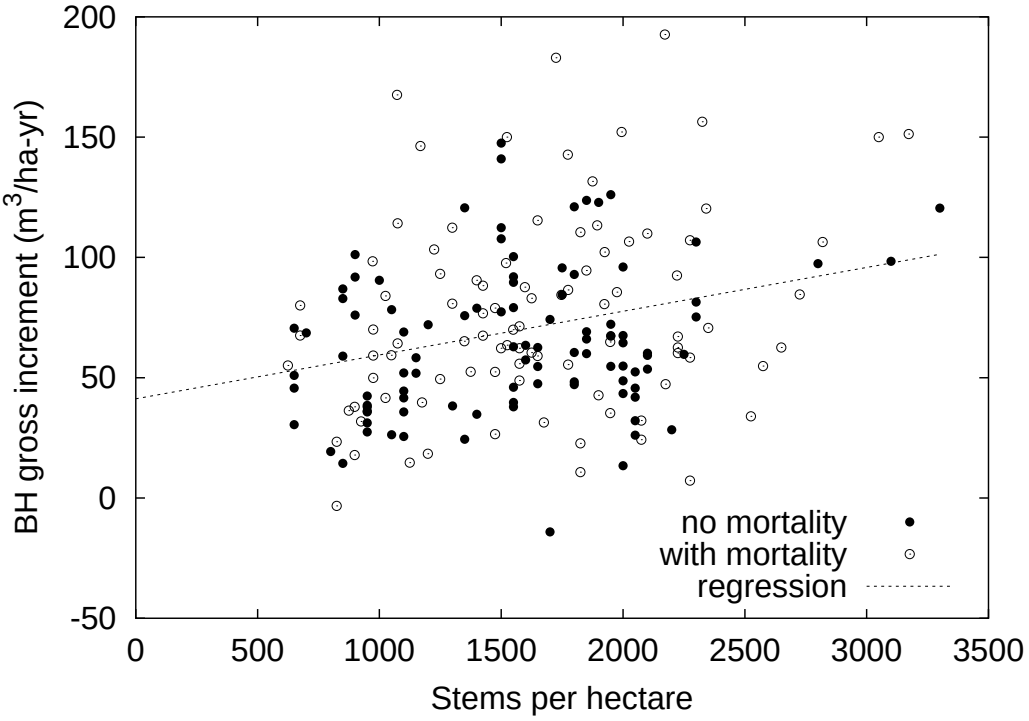

Fig. 8. Calculated gross W increments for "closed" stands ($W > 150$), and fitted regression line.

Coinciding with the radiata pine observations, graphs pointed to N as the best predictor, This was confirmed by running stepwise multiple linear regressions with t, H, B, D and W, in addition to N and various transformations of it: $\ln N$, $1/N$, $\sqrt{N}$, $1/\sqrt{N}$, $N^{0.75}$ and $N^{-0.75}$. The best fit (minimum standard error) was obtained with the simple regression

$$\text{gross increment } = 41.23 + 0.01820N \ , \tag{10}$$

with a standard error of 34.97 and $r = 0.274$.

Other regressions of the form $\alpha + \beta N^\gamma$ were only slightly worse, including the one with the average spacing mentioned before ($\gamma = -1/2$). For more generality in the results, in what follows we write the gross increment in this form.

Substituting in (9), we finally have

$$\frac{\mathrm{d}W}{\mathrm{d}t} = \alpha + \beta N^\gamma - kmW \ , \tag{11}$$

with $\alpha = 41.23$, $\beta = 0.01820$, and $\gamma = 1$.

After substituting N from (7), this is a linear differential equation in W that can be integrated according to standard formulae, giving

$$\begin{aligned} W = {} & \mathrm{e}^{-km(t-t_0)}\, W_0 + \frac{\alpha}{km}[1 - \mathrm{e}^{-km(t-t_0)}] \\ & - \frac{\beta N_0^\gamma}{m(\gamma - k)}[\mathrm{e}^{-\gamma m(t-t_0)} - \mathrm{e}^{-km(t-t_0)}] \ . \end{aligned} \tag{12}$$

The basal area can be recovered from $B = W/H$. It may be more convenient, however, to arrange computations as described in the next section.

7 Closed-stand growth summary and computations

We have described the stand, at any adjusted age t (i. e., the real age multiplied by 7*b*), by three state variables: H, N, and B. The rate of change of these variables (growth, mortality) is given by the differential equations (1), (6), and (11), which can be written as

$$\frac{\mathrm{d}H^c}{\mathrm{d}t} = -\frac{1}{7}H^c + \frac{a^c}{7}$$

$$\begin{aligned}\frac{\mathrm{d}N^{\gamma}}{\mathrm{d}t} &= -\gamma m N^{\gamma} \\ \frac{\mathrm{d}BH}{\mathrm{d}t} &= -kmBH + \beta N^{\gamma} + \alpha\end{aligned} \tag{13}$$

The parameter values are: $a = 31.60$, $c = 0.6339$, $\gamma = 1$, $m = 0.0281$, $k = 0.75$, $\alpha = 41.23$, and $\beta = 0.01820$.

Conceptually, it may be clearer to use differential equations in terms of the basic state variables. Expanding the derivatives on the left-hand side, and after some algebraic manipulation,

$$\begin{aligned}\frac{\mathrm{d}H}{\mathrm{d}t} &= 2.012H^{0.3661} - 0.2254 \\ \frac{\mathrm{d}N}{\mathrm{d}t} &= -0.0281N \\ \frac{\mathrm{d}B}{\mathrm{d}t} &= 0.2043B + 41.23\frac{1}{H} + 0.0182\frac{N}{H} - 2.012\end{aligned} \tag{14}$$

Given an initial state $[H_0, N_0, B_0]$ at the (site-scaled) age t_0, (14) can be numerically integrated to predict the state $[H, N, B]$ at any other age t. Site scaling is achieved by multiplying the actual age by $7b$, with b from (4). Other variables of interest ("outputs"), such as volume per hectare V and mean dbh D, are calculated as functions of the current state variables.

For teaching and training purposes we have found it useful to implement these equations in a visual modelling system such as Vensim, Stella, Powersim, or Dynamo (Figure 9). These are based on Forrester's System Dynamics diagrams, representing state variables by boxes (*levels, stocks*), derivatives by thick arrows with control "valves" (*rates, flows*), and the dependency of rates on state variables by curved arrows (e. g. Ford, 1999). For any initial conditions the system evolution is simulated through numerical integration, and trajectories for the various variables can be displayed in graphical or tabular form.

It is more efficient and accurate, however, to compute predictions through analytical integration. Integrals have already been given in (2), (7), and (13).

Computations can be arranged in a somewhat more convenient form by noting that (13) is a system of linear differential equations in the transformed variables H^c, N^{γ}, and BH. In fact, it is a special case of the multivariate Richards model, where the transformations are more generally products of powers of the basic variables, and their exponents can be parameters to be estimated from the data (García, 1984, 1994; Vanclay, 1994). A common way of solving such a linear system is by "un-coupling" the equations through an eigenvalue-eigenvector transformation. Here we need just one transformed component of

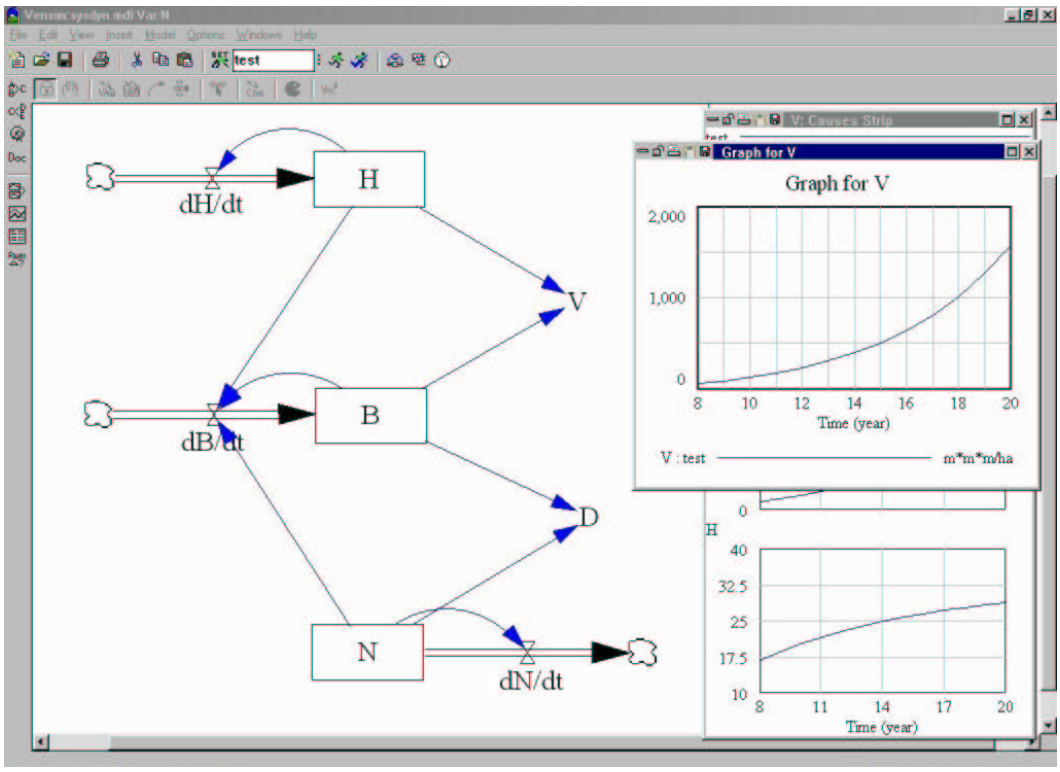

Fig. 9. Simulation of (14) with the free version of Vensim (`www.vensim.com/venple.html`). The simple stand volume equation $V = BH/3$ has been used here.

the form $BH + pN^\gamma$, where p is such that

$$\frac{\mathrm{d}}{\mathrm{d}t}(BH + pN^\gamma) = -km(BH + pN^\gamma) + \text{constant} \; .$$

It is found that $p = -\frac{\beta}{m(\gamma - k)}$. Defining

$$\begin{aligned} x &\equiv a^c - H^c \\ y &\equiv N^\gamma \\ z &\equiv \frac{\alpha}{km} - BH + \frac{\beta}{m(\gamma - k)} N^\gamma \; , \end{aligned} \tag{15}$$

we can then write three independent equations:

$$\begin{aligned} \frac{\mathrm{d}x}{\mathrm{d}t} &= \frac{1}{7}\, x \\ \frac{\mathrm{d}y}{\mathrm{d}t} &= -\gamma m\, y \\ \frac{\mathrm{d}z}{\mathrm{d}t} &= km\, z \; , \end{aligned}$$

and the general solution

$$
\begin{aligned}
x &= \mathrm{e}^{\frac{1}{7}(t-t_0)}\, x_0 \\
y &= \mathrm{e}^{-\gamma m(t-t_0)}\, y_0 \\
z &= \mathrm{e}^{km(t-t_0)}\, z_0 \ .
\end{aligned}
\tag{16}
$$

The calculation procedure consists then of computing the initial x_0, y_0 and z_0 from the initial conditions with (15), projecting these values with (16), and recovering the original state variables from the inverse of (15):

$$
\begin{aligned}
H &= (a^c - x)^{1/c} \\
N &= y^{1/\gamma} \\
B &= (\frac{\alpha}{km} + \frac{\beta}{m(\gamma - k)} y - z)/H \ .
\end{aligned}
\tag{17}
$$

Note that when simulating for a series of equally spaced (e. g., annual) time steps, the factors in (16) only need to be computed once.

8 Initial growth

The basal area growth and mortality predictions seem reliable for BH greater than some 100 to 150 m^3/ha (V greater than 33 to 50 m^3/ha, approximately). Different relationships apply to young stands that have not yet reached these stocking levels. To deal with them, for instance when simulating the development of future stands, we can use a separate (static) model to estimate appropriate starting points for initializing the growth projections. An alternative combined modelling of open and closed stands is presented in the Appendix, but the simpler approach described here was preferred for the practical application.

We chose to estimate H, N, B and t for the time when $BH = 150$. Knowing t, the top height can be obtained from (2). Lacking any better information, (7) may be applied to the initial density (there was no data on the initial densities for the available sample plots), or in a specific situation there might be some more direct estimate for N near age t. What is needed then, is the t at which $BH = 150$ for various values of N.

To estimate this relationship between t and N, we used the first measurement with $BH \geq 150$ in each plot, extrapolating to the initial N and to $BH \equiv W = 150$ with (7) and (13). It is not possible to solve explicitly for t in (13),

Table 2
Starting point regressions

$BH <$	n	best	R	b_0	b_1	SE	$\bar{t}$	SE($\bar{t}$)	SE(b_0)
200	25	$1/\sqrt{N}$	0.625	4.256	117.4	0.772	6.97	0.772	—
250	40	$\ln N$	-0.528	16.52	-1.247	0.739	7.13	0.858	0.326
300	49	$\ln N$	-0.518	17.38	-1.360	0.798	7.09	0.923	0.328
400	63	$\ln N$	-0.510	17.57	-1.399	0.825	6.96	0.951	0.302
500	73	$\ln N$	-0.464	18.48	-1.524	0.985	6.92	1.104	0.345
600	83	$\sqrt{N}$	-0.306	9.144	-0.0520	1.191	6.80	1.244	—
∞	96	$1/N^2$	0.145	6.671	848.9	1.297	6.93	1.307	—

so that in each instance t was calculated numerically by the bisection method. The values thus obtained are shown in Figure 10.

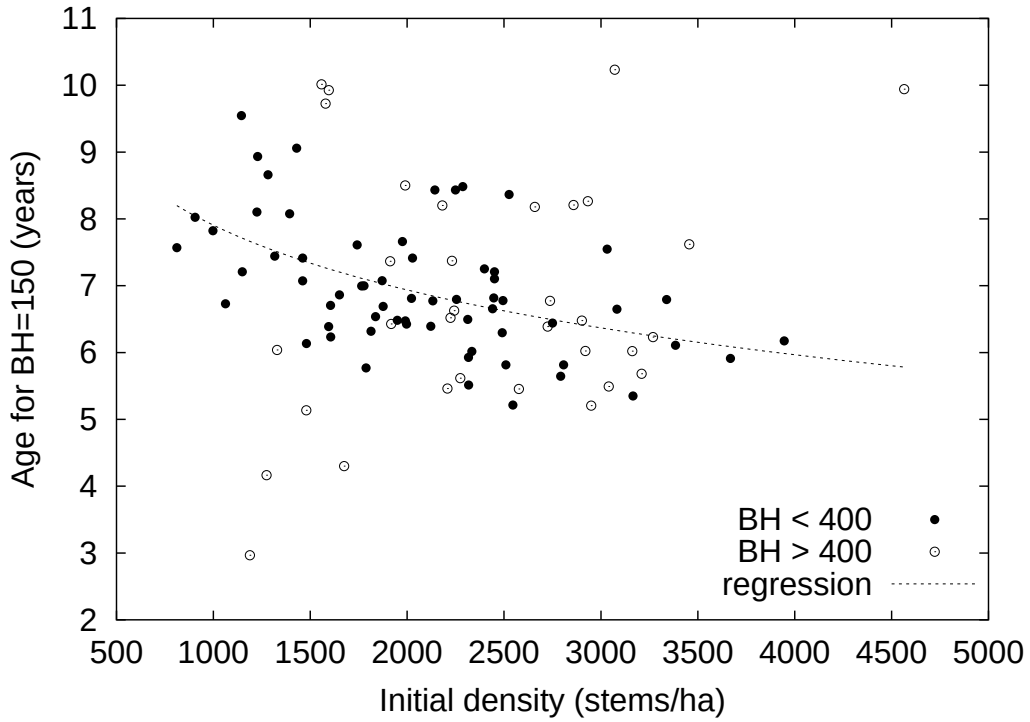

Fig. 10. Projected initial density N and t for $BH = 150$, using the first measurement with $BH \geq 150$ in each plot. Points with observed BH greater or less than 400 are distinguished with different symbols. The curve corresponds to equation (18).

We computed linear regressions of t over N, N^2, $\sqrt{N}$, $1/N$, $1/N^2$, $1/\sqrt{N}$, and $\ln N$. Values farther from $BH = 150$ are obviously less reliable but, on the other hand, excluding them reduces the available number of points. The results from the best regressions for various thresholds are shown in Table 2.

Except for the extreme sample sizes, $\ln N$ was the transformation most highly

correlated with t. The standard error (SE) was not reduced by including additional regressors. As expected, the variability, reflected in higher standard errors and lower correlation coefficients (R), increases with the degree of extrapolation, although the larger sample size compensates to some extent in the precision of the parameter estimates (e. g., S_{b_0}). The consistency of the means, $\bar{t}$, suggests an absence of substantial biases. From a practical point of view the differences between the various regressions are relatively small, and it was decided to use the one obtained for $BH < 400$:

$$t = 17.57 - 1.399 \ln N \tag{18}$$

(Figure 10). Here t is the (site-adjusted) age at which $BH = 150$ is reached for various initial densities N. If N is known at some other age, the initial density (at $t = 0$) may be calculated with (7).

9 Auxiliary relationships

9.1 Volume

The growth model, in the strict sense, projects the changes in state variables due to stand development. Other variables of interest (outputs) can be calculated or estimated from the current state. For instance, the mean (quadratic) dbh, $D = 200\sqrt{B/(\pi N)}$ cm, is calculated easily enough. Estimates for the total volume per hectare are given here. Additional outputs could include merchantable volumes, and dbh distribution parameters (García, 1984).

To reduce the effects of heteroscedasticity we used the volume-basal area ratio V/B as the dependent variable in stepwise linear regression. Various combinations of B and H commonly found in stand volume functions were tried as independent variables: H, $1/B$, H/B. In order to avoid before/after thinning inconsistencies, it is advisable to take also into account the number of stems (Beekhuis, 1966; García, 1984). Accordingly, terms containing N found significant in García (1984) and in later models were added: N, H/N, $H/\sqrt{N}$, NH/B.

There were 388 observations. The regression $V/B = -0.7394 + 0.3334H$, of the form used by Beekhuis (1966), had a standard error (SE) of 0.431. Without the intercept we obtained $V/B = 0.3318H$, with SE= 0.466, essentially the same error than with $V/B = H/3$, confirming the simple approximation $V \approx BH/3$ mentioned before. The SE decreased to 0.274 when a term in N was included:

$$V/B = 0.7723 + 0.3334H - 0.0004361HN/B \ .$$

Up to 6 "significant" terms were found, giving an SE of 0.234. The following intermediate solution, with SE= 0.237, may be a reasonable compromise:

$$V/B = 0.3542 + 0.3332H - 0.0004276HN/B + 0.4958H/B - 3.415/B \ .$$

We decided, however, to use instead the previous two-term function, being simpler and sufficiently precise for our purposes. The estimated volume will then be

$$V = 0.7723B + 0.3334BH - 0.0004361HN \ . \tag{19}$$

9.2 Thinning

Although the data came from unthinned stands, in principle the nature of the model allows predictions of stand development under various thinning regimes. Thinning just causes an instantaneous change in the state variables, and the model can calculate trajectories starting from the new after-thinning state. Obviously, the predictions may be unreliable for states not represented in the data. Also, there may be some over prediction with heavy thinnings, where for some time after the treatment there is less than full occupancy of the site (García, 1990), especially if BH is reduced to less than about 100 m^3/ha. In addition, possible damages from logging or windthrow are ignored. With all these caveats, and accepting that the results will be largely speculative, thinning simulations can be useful.

Often, thinnings are specified in terms of numbers of trees per hectare left or removed, and the corresponding basal area needs to be estimated (it can be assumed that the top height does not change for thinnings from below). Sometimes it is the basal area which is given, possibly as a percentage, and the numbers have to be estimated.

The relationship between number of stems and basal area removed or left in a thinning depends, among other things, on its selectivity. There is no data on this for eucalypts in Galicia. Therefore we used experiences from elsewhere to include in the growth simulator a relationship to calculate thinnings, if necessary. It represents "typical" thinning from below, and its use may be avoided by specifying both thinning basal area and number of stems.

Beekhuis (1966) presents in his Table 4 data on percentage of basal area removed for various percentages of stems removed, for thinnings in *Pinus radiata*. The values vary somewhat between successive interventions, and with the age of thinning, but the following expression gives a reasonable approximation:

$$p_B = 100 - (100 - p_N)^{0.75} \ ,$$

where p_B is the percentage of basal area and p_N the percentage of stems removed. In terms of the basal areas and numbers before and after thinning, B_0, N_0 and B, N, respectively, we get:

$$B/B_0 = (N/N_0)^{0.75} \ . \tag{20}$$

This agrees with the relationships for natural mortality found before. A similar model was used by Elliott and Goulding (1976), and it is a special case of the more general equations of García (1984).

10 Discussion and conclusions

The model was implemented in an interactive computer program. We also provided printed unthinned yield tables, for a range of site indices and initial densities. Extensive testing showed that the model predictions agree well with the measurements, although the variability and limited coverage of the available data indicates that projections should be used with caution. Nevertheless, the rationale behind the equations used, and their basis on experience with other forests, provide a higher level of confidence than what would be expected from a purely empirical model. The approach seems applicable to other data-poor growth modelling situations. It would also be useful to confirm or modify the relationships with more extensive data sets for different species and growing conditions.

It must be remembered that we used data exclusively from first rotation coppice. It is not clear how different the behavior of planted stands could be. Fernández López presents some comparisons between successive coppice rotations in a 1982 unpublished report from the *Centro de Investigaciones Forestales de Lourizán*.

Closure/occupancy models similar to the one in the Appendix may be appropriate when simulation of early and heavy thinnings is important. Pruning effects on growth have also been modelled through these means (García, 1989, 1990).

From a theoretical point of view, perhaps the least satisfactory aspect of this model is the mortality relationship (6). As already pointed out, natural mortality tends to be highly variable, and often does not appreciably deviate from a constant relative rate (see for instance Ferguson and Leech, 1976). Furthermore, in managed stands mortality may be unimportant. Still, it would be interesting to explore alternatives. We believe, however, that analytically integrable models are preferable to those that can only be used through numerical simulation, not only for convenience of use, but also for their potential to

support effective parameter estimation and management optimization procedures. A mortality component compatible with the 3/2 self-thinning rule was used in a growth model for Chilean eucalypts similar to the one described here (O. García, unpublished); although integrable through state variable transformations, recovering the original variables required iteration. A more realistic and tractable mortality modelling remains a challenge.

The multivariate Richards model has been highly successful in summarizing large permanent sample plot data sets, covering a very wide range of treatments (Goulding, 1995). The fact that it encompasses a special case with a mechanistic justification is gratifying, and may partially explain that success.

The parameters could have been re-estimated through more sophisticated simultaneous maximum likelihood techniques developed for the multivariate Richards (García, 1984). Such a refinement was not judged warranted in this instance. In addition, the step-by-step approach seems to present advantages in the incorporation of prior knowledge and subjective data weighting, in a way that would be difficult to achieve with an automated procedure.

Contrary to what might be expected, to make the most of limited information, a higher degree of mathematical and statistical sophistication may be justifiable with scarce data than in data-rich situations.

A Appendix : An extension to open stands

For a more general model, we introduce an additional state variable, R, representing relative closure. One may think of R as the amount of assimilating material as a fraction of that present in a fully closed stand; for instance, in terms of foliage biomass, leaf area index, or some combination of foliage and fine roots. It is unnecessary to be more precise here, it is just an unobserved variable that starts as a small quantity per tree when these are free-growing, and increases up to a maximum of 1 on a hectare basis for a fully closed stand. When thinning, R immediately drops in proportion to the basal area or volume removed, and then gradually recovers.

When $R < 1$, both volume increment and mortality are reduced by an "occupancy factor", Ω, related to R. Top height growth is not affected. It is well-known that moderate thinning has a negligible effect on total increment. Therefore, the relationship between occupancy and closure is non-linear, with $\Omega = 0$ for $R = 0$, $\Omega = 1$ for $R = 1$, and Ω changing little as R nears 1.

We use here a simple special case of the models described in García (1989), where more mathematical details are given. Additional biological justification

and analysis of extensive radiata pine data are presented in García (1990). The right-hand sides of (11) and (6) are multiplied by the occupancy factor

$$\Omega = 1 - (1 - R)^2 = R(2 - R) \tag{A.1}$$

(this is (4) with $m = 2$ or (5) with $a = 2$ in García (1989)). Stand closing is modelled by the logistic

$$\frac{\mathrm{d}R}{\mathrm{d}t} = \theta R(1 - R) \ , \tag{A.2}$$

with the initial condition $R = r_0 N$ at breast-height age [3]. Estimation of the parameters θ and r_0 is described below.

It is clear that this model coincides with the previous one when $R = 1$. For $R < 1$, it is found that it is sufficient to substitute for t in (7) and (13), or in the last two equations of (16), the "physiological time"

$$t + (R - \ln R - 1)/\theta \tag{A.3}$$

(García, 1989). R starts at $r_0 N$ for $H = 1.3$, and is projected with the integral of (A.2):

$$R = 1/\{1 + (1/R_0 - 1)\exp[-\theta(t - t_0)]\} \ . \tag{A.4}$$

When thinning, the current R may be reduced by multiplying by the ratio of residual to current basal area.

We looked for parameter values that would make the predictions of this model as close as possible to those from the segmented approach. With initial densities of 1000, 2000, 3000, and 4000 stems per hectare, we took the ages at which $BH = 150$ ($V \approx 50$ m^3/ha), and the yield table entries with V closest to 100 and 200 m^3/ha. This gave 12 density–age combinations for which we computed predictions with both models; discrepancies at older ages would be expected to be smaller. We used a general-purpose optimization algorithm to minimize sums of squares, and the maximum absolute relative differences, with similar results. The values $\theta = 2.153$ and $r_0 = 5.53010^{-8}$ gave a maximum relative difference in both basal area and number of stems of just under 1%, negligible for all practical purposes.

[3] As a reviewer pointed out, in principle, other state variables might affect (A.2). Possibly just H, because stand density is reflected in R, and there is no obvious causal connection between accumulated stem-wood and growth. The simpler model was sufficient here.

We conclude that this extended model is capable of simulating the growth over the whole range of interest, without the need for a separate initial growth relationship. Compared to the segmented approach it is more flexible, elegant, and potentially more accurate for early and heavy thinnings. However, given the current limited interest in thinning in Galicia, and the added usage and comprehension difficulties due to having to account for R, it was decided not to use it in this instance.

Acknowledgements

The participation of the senior author in this work was funded by the *Empresa Nacional de Celulosas* (ENCE) through the *Fundación del Conde del Valle de Salazar*, while he was a guest professor with the *Escuela Técnica Superior de Ingenieros de Montes* at the *Universidad Politécnica de Madrid*. He is grateful to the University for their hospitality, and especially to Professor Alberto Madrigal for managing the project and providing much support, technical advice, and encouragement. We gratefully acknowledge the collaboration of numerous personnel at ENCE. In particular the advice and support from the Director of Research, Gabriel Toval, and the assistance of Manuel Pardo in facilitating our access to the data and patiently answering many questions.

References

Alder, D., 1980. Forest volume estimation and yield prediction. Vol.2 - Yield prediction. Forestry paper 22/2, FAO.

Assmann, E., 1970. The principles of forest yield study. Pergamon Press.

Bailey, R. L., Clutter, J. L., 1974. Base-age invariant polymorphic site curves. Forest Science 20, 155–159.

Beekhuis, J., 1966. Prediction of yield and increment in *pinus radiata* stands in New Zealand. Technical Paper 49, Forest Research Institute, NZ Forest Service.

Clutter, J. L., Fortson, J. C., Pienaar, L. V., Brister, G. H., Bailey, R. L., 1983. Timber Management: A Quantitative Approach. Wiley, London.

Drew, T. J., Flewelling, J. W., 1979. Stand density management: an alternative approach and its application to Douglas-fir plantations. Forest Science 25, 518–532.

Eichhorn, F., 1904. Beziehungen zwischen Bestandshöhe und Bbestandsmasse. Allgemeine Forst- und Jagdzeitung 80, 45–49.

Elliott, D. A., Goulding, C. J., 1976. The Kaingaroa growth model for radiata pine and its implications for maximum volume production. New Zealand Journal of Forestry Science 6, 187, (abstract).

Ferguson, I. S., Leech, J. W., 1976. Stand dynamics and density in radiata pine plantations. New Zealand Journal of Forestry Science 6 (3), 443–454.

Ford, A., 1999. Modeling the Environment. Island Press, Washington, D. C., Covelo, California.

García, O., 1983. A stochastic differential equation model for the height growth of forest stands. Biometrics 39, 1059–1072.

García, O., 1984. New class of growth models for even-aged stands: *Pinus radiata* in Golden Downs Forest. New Zealand Journal of Forestry Science 14, 65–88.

García, O., 1989. Growth modelling — new developments. In: Nagumo, H., Konohira, Y. (Eds.), Japan and New Zealand Symposium on Forestry Management Planning. Japan Association for Forestry Statistics.

García, O., 1990. Growth of thinned and pruned stands. In: James, R. N., Tarlton, G. L. (Eds.), New Approaches to Spacing and Thinning in Plantation Forestry: Proceedings of a IUFRO Symposium, Rotorua, New Zealand, 10–14 April 1989. Ministry of Forestry, FRI Bulletin No. 151.

García, O., 1994. The state-space approach in growth modelling. Canadian Journal of Forest Research 24, 1894–1903.

García, O., 1995. Indices de sitio preliminares para eucalipto. Ciencia e Investigación Forestal 9 (1), 5–21.

García, O., 1999. Height growth of *Pinus radiata* in New Zealand. New Zealand Journal of Forestry Science 29 (1), 131–145.

Goulding, C. J. G., 1995. Growth and yield models. In: Hammond, D. (Ed.), 1995 Forestry Handbook. New Zealand Institute of Forestry, Christchurch.

Madrigal C., A., Alvarez G., J. G., Rodríguez S., R., Rojo A., A., 1999. Tablas de Producción para los Montes Españoles. Fundación Conde del Valle de Salazar, Escuela Técnica Superior de Ingenieros de Montes, Madrid.

Mitchell, K. J., 1975. Dynamics and simulated yield of Douglas-fir. Forest Science Monograph 17, Society of American Foresters.

Pardo, M., 1990. Forestry management of a Spanish *Eucalyptus globulus* area based on continuous forest inventory. In: Adlard, P., Rondeux, J. (Eds.), Forest Growth Data: Capture, Retrieval and Dissemination. Proceedings of the Joint IUFRO Workshop S4.02.03-S4.02.04 held on 3-5 April 1989 at Gembloux, Belgium. Faculty of Agriculture of Gembloux, Belgium.

Rojo, A., Montero, G., 1994. Tablas de producción españolas. Montes 38, 35–42.

Vanclay, J. K., 1994. Modelling forest growth and yield: Applications to mixed tropical forests. CABI International.